

# Enhancement of the Surface and Bulk Mechanical Properties of Polystyrene Through the Incorporation of Raw Multiwalled Nanotubes with the Twin-Screw Mixing Technique

Sung-Po Liu,<sup>1</sup> Wei-Lun Hsu,<sup>1</sup> Kung-Chin Chang,<sup>2</sup> Jui-Ming Yeh<sup>2</sup>

<sup>1</sup>Department of Mechanical Engineering, Ching Yun University, Chung-Li 32097, Taiwan, Republic of China

<sup>2</sup>Department of Chemistry and Center for Nanotechnology, Chung-Yuan Christian University, Chung-Li 32023, Taiwan, Republic of China

Received 28 May 2008; accepted 8 October 2008

DOI 10.1002/app.29526

Published online 2 April 2009 in Wiley InterScience (www.interscience.wiley.com).

**ABSTRACT:** In this article, we present the effects of incorporated multiwalled nanotubes (MWNTs) on a metal surface and the bulk mechanical properties of as-synthesized polystyrene (PS)–MWNT composites prepared with the twin-screw mixing technique. The MWNTs used for preparing the composites were raw compounds that were not treated with any surface modifications. The morphology for the dispersion capability of the MWNTs in the PS matrix was subsequently characterized with transmission electron microscopy. Surface mechanical property studies (i.e., wear resistance and hardness) showed that the integration of MWNTs led to a distinct increase in the wear resistance and also the micro/nanohardness with up to a 5 wt % MWNT loading in the composites. Moreover, the enhancement of the wear resistance of the as-prepared composites, in comparison with pure PS, was further identified with scanning electron microscopy observations of

the surface morphology after testing. On the other hand, for bulk mechanical property studies (i.e., the tensile strength and flexural strength), the composites containing a 3 wt % concentration of MWNTs in the PS matrix exhibited the best performance with respect to the tensile strength and flexural strength. This means that this composition of MWNTs exhibited good compatibility with the PS matrix, and this can be attributed to the  $\pi$ – $\pi$  interacting forces existing between the aromaticity of the MWNTs and PS matrix. Furthermore, at higher MWNT loadings (e.g., 5 wt %), raw MWNTs were aggregated in the polymer matrix, as observed by transmission electron microscopy. Also, this led to an obvious decrease in the tensile strength and flexural strength. © 2009 Wiley Periodicals, Inc. *J Appl Polym Sci* 113: 992–999, 2009

**Key words:** composites; mechanical properties; polystyrene

## INTRODUCTION

Dr. Sumio Iijima, who was working for Nippon Electronics, discovered carbon nanotubes (CNTs) when he was using the arc-discharge method to study the C60 component and found the deposit from the negative pole component.<sup>1–3</sup> Because CNTs have a higher aspect ratio and a smaller scale and can produce an arrangement that is mainly a graphite net structure, the quality is light, and the axis is high-quality. It is quite suitable as a molecule for strengthening materials, such as polymer bases, ceramic bases, and metal-base composites. CNTs have good elasticity, super-strong mechanical intensity, and low weight characteristics (the specific gravity is only one-sixth of the specific gravity of steel). As a result, they are very

suitable for addition to metals, ceramics, and polymers as enhanced materials of composites unifying high intensity and light mass function are in demand.

CNTs can be applied to the structural bodies of airplanes, sports apparatus, and various kinds of construction materials. The basic structure of CNTs consists of a hexagonal carbon ring, bent and half-ball caps at both ends of the tubes contain some pentagons and heptagons in the structure's carbon ring, and the carbon–carbon covalent bond is a steadier chemical bond in nature, so CNTs have quite good mechanical performance.<sup>4</sup> Because of the reinforcement effects, CNTs can be used to fabricate nanocomposites with excellent tribological properties. The tribological behavior of copper/CNT,<sup>5</sup> carbon/CNT,<sup>6</sup> and phosphorus nickel/CNT composite coatings<sup>7,8</sup> and polyimide/CNT,<sup>9</sup> polytetrafluoroethylene/CNT,<sup>10</sup> and ultrahigh-molecular-weight polyethylene/CNT<sup>11</sup> nanocomposites has been investigated.

On the other hand, polystyrene (PS) comes from the polymerization of styrene monomer. Its relative density is 1.05–1.07, and it has an amorphous structure. The glass-transition temperature is about 80°C, and the

Correspondence to: S.-P. Liu (spliu@cyu.edu.tw).

Contract grant sponsor: National Science Council of Taiwan; contract grant number: NSC 94-2622-E-231-013-CC3.

applicable temperature range is 60–75°C. Because it contains a benzene ring in the molecule, PS can activate the C–H bond of the  $\alpha$  location. This relief, which oxidizes the metric, will produce aging and cracking in air for a long period of time. The other viewpoint is that when glass fiber is used to strengthen PS, the performance will be outstanding, with an improvement in the low-temperature impact toughness.

Recently, the research activities associated with the preparation and property studies of polymer/multiwalled nanotube (MWNT) composites have attracted a great amount of attention. For example, Allaoui et al.<sup>12</sup> studied epoxy resin and MWNT composite materials and, after adding an aged hardener, observed that they had the characteristics of composites with respect to the elasticity and ductility. For example, with the addition of 1 wt % MWNTs, Young's modulus was doubled, and the tensile strength was tripled. Jin et al.<sup>13</sup> studied poly (methyl methacrylate) (PMMA) with MWNTs added for strength. They found that when MWNTs were added, they could increase the storage modulus of the material, and the glass-transition temperature increased. Zeng et al.<sup>14</sup> added carbon nanofibers at 5 and 10 wt % concentrations separately and produced PMMA composites. They found that with the addition of 5 wt % nanocarbon fibers, Young's modulus of the as-prepared composites increased 55%.

Furthermore, there have been several studies focusing on PS–MWNT nanocomposites prepared by *in situ* polymerization,<sup>15,16</sup> *in situ* bulk sonochemical polymerization,<sup>17,18</sup> vacuum casting,<sup>19</sup> and ultrasound-assisted solution vaporation.<sup>20</sup> For example, Qian et al.<sup>20</sup> reported that there were drastic increases in the elastic modulus and fracture strength of PS–MWNT nanocomposites with only a 1 wt % MWNT concentration and that the mechanical properties of the nanocomposites compared favorably with those of polypropylene–carbon fiber (10 wt %) composites. Because MWNTs have superior mechanical properties and a high aspect ratio, they are potential reinforcing agents for PS. However, the effects of incorporated MWNTs on the mechanical properties of PS–MWNT composites have seldom been mentioned. Therefore, in this work, we studied the effect of the addition of MWNTs on the surface mechanical properties (e.g., wear resistance and micro/nanohardness) and bulk mechanical properties (e.g., tensile strength and flexural strength) of as-prepared composites. Transmission electron microscopy (TEM) was used to investigate the dispersion capability of MWNTs in the PS composites. Furthermore, the enhanced wear resistance of the as-prepared composites versus that of pure PS was further identified by scanning electron microscopy (SEM) observation of the surface morphology of the as-prepared samples after testing.

## EXPERIMENTAL

### Chemicals and instrumentation

MWNTs with a length of 5–15  $\mu\text{m}$  and a diameter of 40–60 nm were purchased from Desunnano Co. (Taipei, Taiwan). The purity of the pristine MWNTs used in this research was 95%. PS (model PG33 with a high weight-average molecular weight of 350,000) was purchased as pellets from Qimei Stock Co. (Tuinan, Taiwan). The samples for the TEM study were prepared by the placement of the PS–MWNT composite material powder into epoxy resin capsules followed by the curing of the epoxy resin at 100°C for 24 h in a vacuum oven. Then, the cured epoxy-resin-containing PS–MWNT composite materials were microtomed with a Reichert-Jung Ultracut-E (Reichert Microscope Services, USA) into 60–90-nm-thick slices. Subsequently, a layer of carbon about 10 nm thick was deposited onto these slices on 300-mesh copper nets for TEM observations on a JEOL 200FX (Tokyo, Japan) with an acceleration voltage of 120 kV. SEM with a Hitachi S-4100 (Tokyo, Japan) model field emission scanning electron microscope was used to evaluate the surface morphology of the as-prepared composite materials.

A Plastograph mixer machine (model PLE-331 corotating, nonintermeshing machine with a maximum screw speed of 120 rpm, a length/diameter ratio of 32, a test temperature range of 20–400°C, and a maximum chamber volume of 50 g) and a hot-press machine (model FC-60 TON), manufactured by Brabender Machine Co. (Ohg, Duisburg, Germany) and Long-Chung Co. (Tuinan, Taiwan), respectively, were used to make the as-prepared samples in the standard shape. The tensile and flexural testing of the PS–MWNT specimens was carried out with universal testing instruments manufactured by Hong-Da Co. (Taichung, Taiwan; model HT-9102). The micro/nanohardness tests were run on an Ulte-Micro model UMIS2 indentation tester from CSIRO Co. (Hobart, Australia) for high- and low-hardness samples, respectively, with an indentation time of 10 s at 25°C. The wear resistance tests were run on a wearing test machine from Taber Co. (model 5130 abrader, USA).

### Preparation of the PS–MWNT composite materials with the twin-screw mixing technique

Before the blending, PS and MWNTs were dried at 90°C in a vacuum oven for 1 h. PS–MWNT composites were prepared in a Plastograph mixer machine twin-screw extruder at 210°C with screw speeds of 65 rpm for 6 min of blending and 75 rpm for 4 min of blending; the total blending time was 10 min.

The melt-mixing procedure for the PS–MWNT composites was performed by the repeated blending

of the samples (at least twice) to produce products in pellet form with better combinations. The as-prepared PS–MWNT composite pellets were subsequently mixed with the Plastograph machine by the twin-screw mixing method to obtain nanocomposites with standard-shape specimens for the following investigations. The melt-mixing procedure of PS–MSWNTs composites was performed by blending samples repeatedly, at least twice, to form products in the shape of pellets, with better combinations. The as-prepared PS–MWNTs composite pellets were subsequently mixed by a Plastograph-Mixer using the twin-screw mixing method to obtain nanocomposites with standard shaped specimens for the following investigations. Melt mixing is a procedure in which the mixture's consistency is an important step in the polymer material processing. Using mechanical force to blend is the most convenient and practical method. It can also change the quality of high polymers through melting technology effectively. It is one of the most frequently used methods in the industry.<sup>13</sup>

#### **Hot pressing of the PS–MWNT composite materials**

According to the test standard of the experimental project, we designed the mold for the hot-pressing requirement and then used the hot-press machine for the tests. The mold was placed under a pressure of 150 kg/cm<sup>2</sup> at 210°C. The pressure was held for 3 min, and the leak pressure was held for 30 s. This test was repeated three times, and the mold was taken out after the hot pressing was finished. Then, the mold was allowed to cool to room temperature, and the mold was opened so that the specimen could be taken out.

#### **Testing of the surface mechanical properties**

##### **Wear resistance testing**

Wear resistance is one of the most convenient and basic properties of a material undergoing mechanical property testing. When one object is being used and is in contact with other objects for a long time, wearing will occur. Therefore, it is necessary to perform a long-period wear–tear test. This experiment uses wearing test machines to determine a material's roll wear and slip wear and then show the decreasing ability of this material's surface to resist wear.

##### **Micro/nanoindenter testing**

We used an Australia UMIS nanoindenter as the depth-detect instrument for our nanohardness testing, and we selected triangular awl modeling (Berkovich) for the investigation. Because of the detection equipment's accuracy and sensitivity for micro/nanohardness tests, the temperature and humidity of the

environment were controlled, and the antivibration was also considered. We held the hardness-measuring apparatus and used the ceramic board for heating on the first appearance. We then put thermal glue on the inserted hold base and kept the experimental specimen parallel to the horizontal plane to ensure that the examination was performed in the vertical accuracy of the moving direction (*z* direction); then, the micro/nanohardness measurements could be carried out after the inserted hold base cooled.

#### **Test of the bulk mechanical properties**

##### **Tensile strength testing**

Among mechanical properties, the tensile strength is one of the most frequently used for comparison. The testing of the tensile strength involves the exertion of the greatest tensile stress and an attempt to extract the test piece before cracking (or plastic deformation). In this experiment, according to the ASTM D 638 standard, the material should be shaped into a dumb-bell-shaped specimen first, and then the tensile test is carried out. At least five specimens are examined in each group, the average is calculated, and the greatest strength of the tensile tests is recorded.

##### **Flexural strength testing**

The flexural test can measure the deformation energy or fracture strength that bears the bending moment for the tested materials. In general, there are three kinds of measurement methods for flexural tests: cantilever, three-point, and four-point. It is common to use the three-point method for measurements in laboratories. This method places the test specimen on two fixed displacements, and force is applied at the central point with a certain pressing speed until the test specimen fractures. The flexural test can be used to determine Young's modulus. Also, the experiment is performed according to the ASTM D 790 standard.

## **RESULTS AND DISCUSSION**

#### **TEM observations of the PS–MWNT composite materials**

In this study, raw MWNTs were added to the PS matrix through the twin-screw mixing technique. TEM was further used to observe the dispersion capability of the MWNTs in the as-prepared composites. As shown in Figure 1(a), we found that a 3 wt % concentration of MWNTs showed good dispersion capability in the PS matrix. The good compatibility between the two phases can be attributed to the  $\pi$ – $\pi$  interaction forces existing between the aromaticity of the MWNTs and PS matrix.

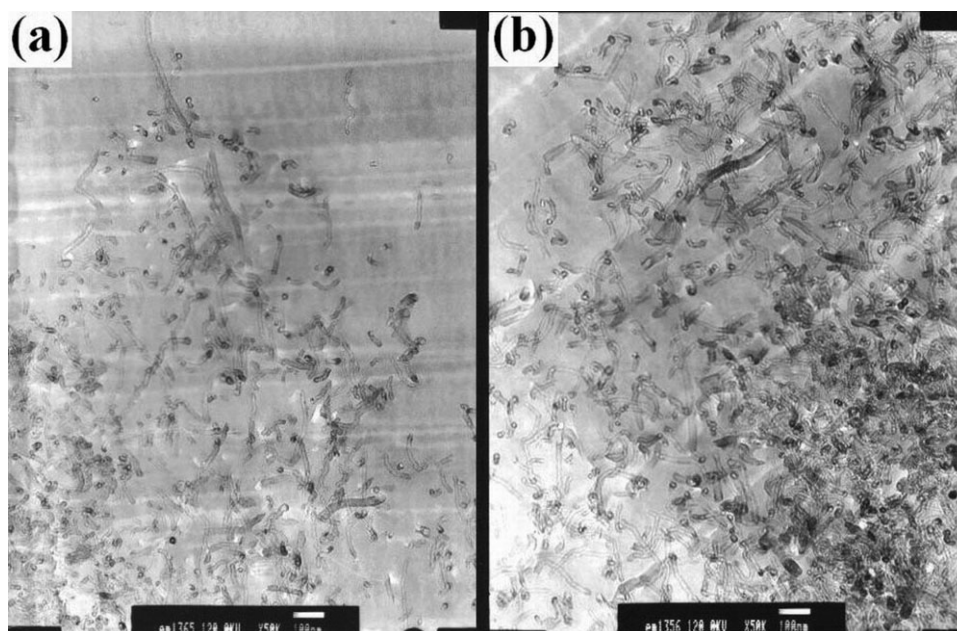


**Figure 1** TEM images of PS–MWNT composites with (a) 3 wt % MWNTs (50,000 $\times$ ) and (b) 5 wt % MWNTs (50,000 $\times$ ).

Furthermore, a 5 wt % concentration of MWNTs also showed good dispersion capability in the polymer matrix. However, an overdose of the MWNT loading embedded in the as-prepared composites may have caused the observable aggregation of MWNT clusters in the polymer matrix, as shown in Figure 1(b). The different dispersion morphology of MWNTs in the polymer matrix could have led to the as-prepared composites revealing different mechanical properties. For the property studies, the discussed mechanical properties can be categorized into two types: surface mechanical properties (e.g., wear resistance and micro/nanohardness) and bulk mechanical properties (e.g., tensile strength and flexural strength).

### Surface mechanical property studies

#### Wear resistance testing

Test specimens with dimensions of  $100 \times 100 \times 2.8 \text{ mm}^3$  were made. After that, a wearing test machine with a load of 1000 g was used to measure the wear loss at wearing speeds of 500 and 1000 rpm to probe the wear resistance properties of the as-prepared composites.

Figure 2 shows the wear loss of the as-prepared pure PS and PS–MWNT composites. For example, the amount of wear loss at 500 rpm for the as-prepared composites was found to slightly increase from the original 63.94 mg for PS to 58.04 mg for PSCNT5. This indicated that the wear loss of the as-prepared composites was reduced slightly as the content of MWNTs in the composites increased at

the low wearing speed of 500 rpm. Moreover, at the higher wearing speed of 1000 rpm, the wear loss of the as-prepared composites was found to decrease significantly. For example, the amount of wear loss for the composites changed from the original value of 128.74 mg for PS to 111.41 mg for PSCNT5, as summarized in Table I. This implied that the higher content of MWNTs (e.g., 5 wt %) in the composites led to a reduction in the wear loss at the higher wearing speed, reflecting that the incorporation of MWNTs into PS might have led to better wear resistance for the as-prepared samples.

Moreover, the wear resistance of the as-prepared composites could be further evaluated by the visual

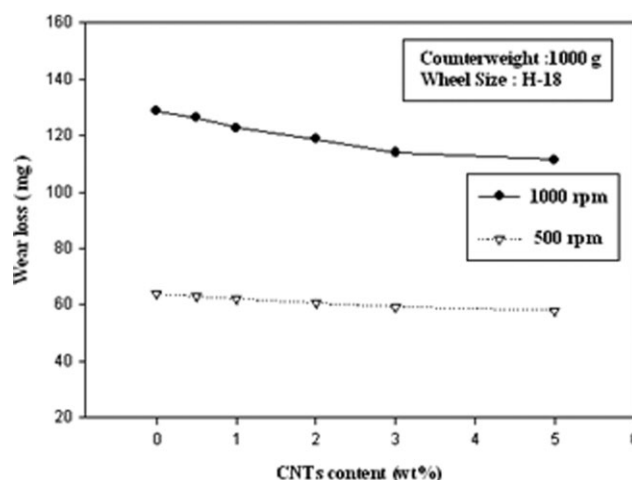


**Figure 2** Effect of the CNT content on the wear loss of PS–MWNT composites.

**TABLE I**  
**Relationship of the Composition of PS–MWNT Nanocomposite Materials with the Mechanical Properties**

Compound composition	Feed code (wt %)		Tensile strength (MPa)	Flexural strength (MPa)	Micro/nanohardness (Hv)	Wear loss (mg)
	PS	MMT				
Ps	100	0	27.56	9.25	18.38	128.74
PsCNT0.5	99.5	0.5	27.95 (+1.42%)	92.48 (+1.95%)	19.19 (+4.41%)	126.27 (−1.92%)
PsCNT1	99	1	28.54 (+3.56%)	95.71 (+5.51%)	20.38 (+10.88%)	122.71 (−4.68%)
PsCNT2	98	2	30.60 (+11.03%)	101.40 (+11.78%)	21.34 (+16.10%)	118.83 (−7.70%)
PsCNT3	97	3	34.42 (+24.56%)	122.29 (+34.81%)	22.85 (+24.32%)	113.96 (−11.48%)
PsCNT5	95	5	33.44 (+21.35%)	118.66 (+30.81%)	23.16 (+26.01%)	111.41 (−13.46%)

observation of the as-prepared composites after the wearing test. Figure 3(a–c) shows SEM images of pure PS, PSCNT2, and PSCNT5, respectively.

SEM observation of the pure PS morphology revealed an uneven and rough surface, indicating that the pure PS had soft surface structures. After the wearing test, the material structures of the pure PS could be easily degraded and removed from the surface of the as-prepared sample, as shown in Figure 3(a). However, the surface morphology of the PS–MWNT composites displayed a relatively smooth pattern in comparison with the pure PS, as illus-

trated in Figure 3(b,c). This implied that the incorporation of MWNTs into PS might have effectively enhanced the wear resistance of PS. This conclusion, obtained from the SEM observations, was consistent with previous studies related to wear loss measurements of pure PS and corresponding composites. The increase in the surface wear resistance of pure PS by the incorporation of MWNTs can be attributed to the increase in the surface hardness of the pure polymer by the introduction of MWNTs. Schadler et al.<sup>21</sup> reported that load transfer to nanotubes in epoxy composites is much higher in compression.

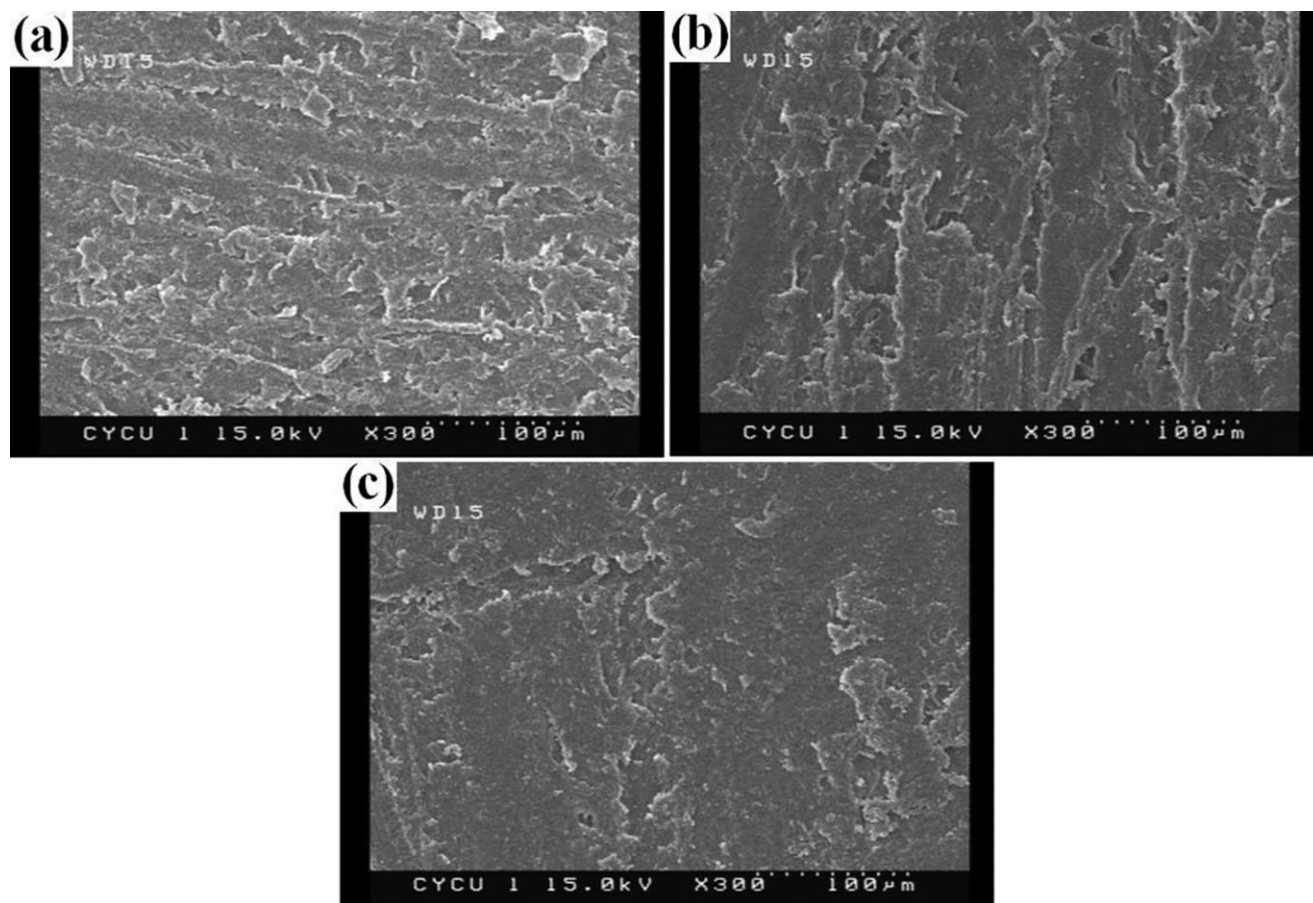


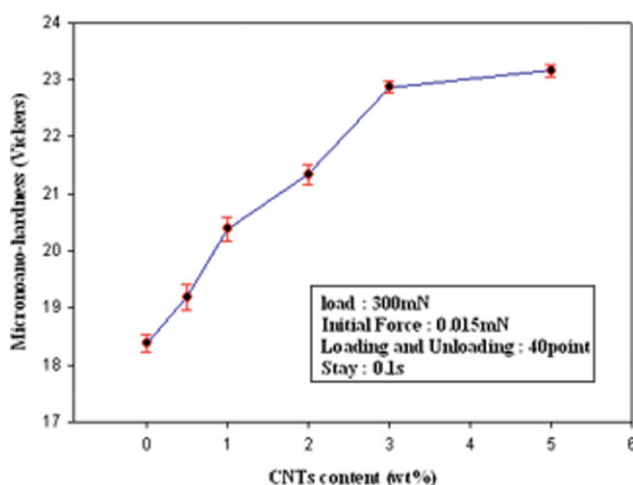
**Figure 3** SEM images of typical worn surfaces of (a) pure PS and (b) PSCNT2 and (c) PSCNT5 nanocomposites.

The addition of MWNTs might contribute to increases in the local compressive and shear strength. Because the strengthening effect of MWNTs with a weight percentage of 3% as reinforcing agents reaches the maximum, the changing tendency of the mechanical and wear properties of the nanocomposites comes to a critical turning point at this MWNT concentration.<sup>22</sup> This finding can be further supported by micro/nano-hardness measurements of the composites, as discussed in the following sections.

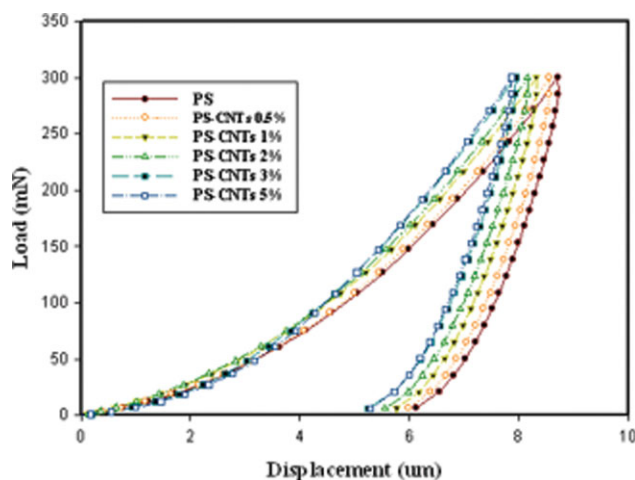
#### Micro/nanoindenter testing

Figure 4 shows the micro/nano-hardness measurements of pure PS and corresponding PS–MWNT composites. As the MWNT content increased, the corresponding micro/nano-hardness value of the composites increased up to a 5 wt % MWNT loading in the composites, as summarized in Table I. For example, the pure PS showed a low surface hardness of 18.38 Hv. Once raw MWNTs were added to PS, the surface hardness increased to 20.38 Hv for PSCNT1, 21.34 Hv for PSCNT2, and 23.16 Hv for PSCNT5. This indicated that the surface hardness of the composite materials increased with increasing MWNT content. Thus, the integration of raw MWNTs into the PS matrix did indeed change the surface characteristics of the composite materials significantly according to the surface mechanical property studies.

Figure 5 shows the micro/nano-hardness indenter displacement obtained for pure PS and its composites. With the greatest amount of indenter displacement, when the PS base was loaded to the maximum and unloaded to the finish, the hardness was worst. When the MWNT content in the compos-



**Figure 4** Micro/nano-hardness of PS–MWNT composites as a function of the CNT content. [Color figure can be viewed in the online issue, which is available at [www.interscience.wiley.com](http://www.interscience.wiley.com).]



**Figure 5** Variation of the load of PS–MWNT composites with the displacement. [Color figure can be viewed in the online issue, which is available at [www.interscience.wiley.com](http://www.interscience.wiley.com).]

ite materials was increased gradually, the amount of indenter displacement changed and moved to the left; this meant that the amount of displacement decreased. When a 5 wt % concentration of MWNTs was added to the composite materials, the amount of indenter displacement was the least, and this revealed that the hardness value of PSCNT5 was the highest. This conclusion is consistent with previous studies associated with surface hardness evaluations.

#### Bulk mechanical property studies

##### Tensile strength testing

Relationships between the tensile properties and MWNT loading, as obtained from tensile tests of

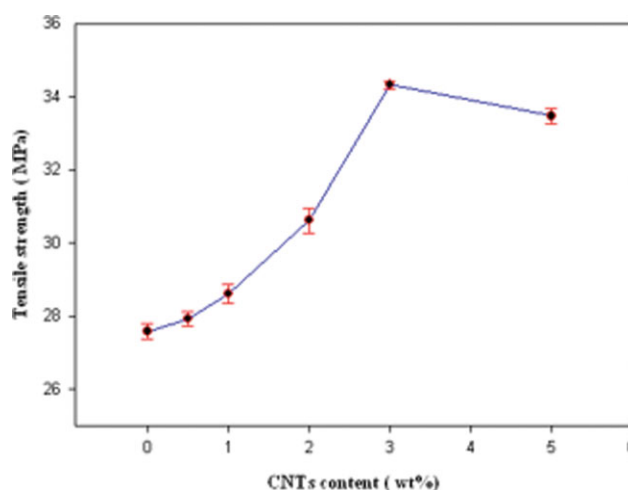


**Figure 6** Tensile strength of PS–MWNT composites as a function of the CNT content. [Color figure can be viewed in the online issue, which is available at [www.interscience.wiley.com](http://www.interscience.wiley.com).]

standard dumbbell-shaped PS–MWNT composite materials, were studied, as shown in Figure 6. For example, upon the addition of MWNTs into PS, the tensile strength of the composites increased to 27.95 MPa for PSCNT0.5, 28.54 MPa for PSCNT1, and 34.42 MPa for PSCNT3. Furthermore, an overdose of the MWNT loading (e.g., 5 wt %) in the composites was found to reduce the tensile strength of the as-prepared composite materials, as summarized in Table I. This indicated that the introduction of MWNTs into the polymer matrix effectively affected the tensile properties of pristine PS. However, the decrease in the tensile strength for PSCNT5 probably resulted from the aggregation of MWNTs in the composites. Similar trends were also found for the flexural strength of the as-prepared composites.

#### Flexural strength testing

Relationships between the flexural strength and MWNT loading, as obtained from tensile tests of standard dumbbell-shaped PS–MWNT composite materials, were studied, as shown in Figure 7. For example, upon the addition of MWNTs into PS, the flexural strength of the composites increased to 92.48 MPa for PSCNT0.5, 95.71 MPa for PSCNT1, and 122.29 MPa for PSCNT3. Furthermore, an overdose of the MWNT loading (e.g., 5 wt %) in the composites was found to reduce the tensile strength of the as-prepared composite materials, as summarized in Table I. This indicated that the introduction of MWNTs into the polymer matrix effectively affected the flexural properties of pristine PS. However, the decrease in the flexural strength for PSCNT5 probably resulted from the aggregation of MWNTs in the composites.

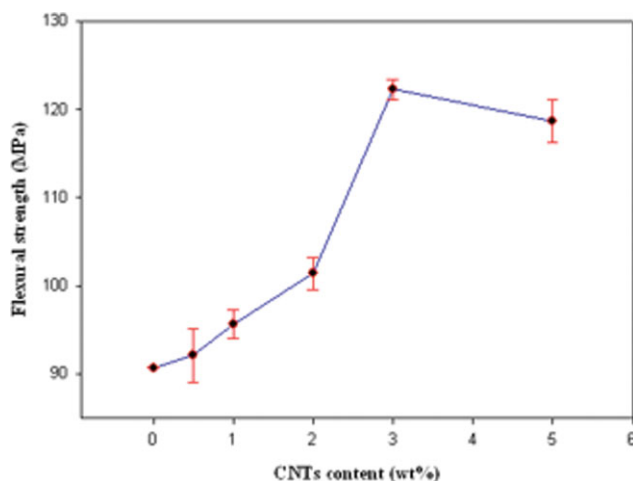


**Figure 7** Variation of the flexural strength of PS–MWNT composites with the CNT content. [Color figure can be viewed in the online issue, which is available at [www.interscience.wiley.com](http://www.interscience.wiley.com).]

## CONCLUSIONS

In this article, we have presented the effects of integrated MWNTs on the surface and bulk mechanical properties of as-synthesized PS–MWNT composites prepared with the twin-screw mixing technique. The MWNTs employed to prepare the composites were raw compounds without any surface modifications. The morphology for the dispersion capability of the MWNTs in the PS matrix was subsequently characterized with TEM. We found that a 3 wt % MWNT loading showed good dispersion capability in the PS matrix on the basis of TEM observations. Moreover, a 5 wt % MWNT loading also showed good dispersion capability in the PS matrix. However, some domains of the TEM micrograph also showed that MWNT clusters combined.

The mechanical studies could be divided into surface and bulk types. In the studies of the surface mechanical properties (e.g., wear resistance and micro/nanohardness), we found that the integration of MWNTs exhibited a distinctly increasing trend for wear resistance and micro/nanohardness up to a 5 wt % MWNT loading in the composites. Moreover, the enhancement of the wear resistance of the as-prepared composites versus the pure PS was further verified by SEM observation of the surface morphology of the as-prepared samples after testing.

On the other hand, for the bulk mechanical property studies (i.e., tensile strength and flexural strength), we found that the composites containing a 3 wt % concentration of MWNTs in the PS matrix exhibited the best performance with respect to the tensile strength and flexural strength. This implied that for this type of composition, MWNTs exhibited good compatibility with the PS matrix, and this could be attributed to the  $\pi$ – $\pi$  interaction forces between the aromaticity of the MWNTs and the PS matrix. Furthermore, at higher MWNT loadings (e.g., 5 wt %), the raw MWNTs were found to be aggregated in the polymer matrix, as observed by TEM, and this led to an obvious decrease in the tensile and flexural strength.

## References

1. Iijima, S. *Nature* 1991, 354, 56.
2. Oberlin, A.; Endo, M. *J Cryst Growth* 1976, 32, 335.
3. Nesterenko, A. M.; Kolesnik, N. F.; Akhmatov, Y. S.; Sukhomlin, V. I.; Prilutski, O. V. *News Acad Sci USSR* 1982, 3, 12.
4. Baughman, R. H.; Zakhidov, A. A.; de Heer, W. A. *Science* 2002, 297, 787.
5. Tu, J. P.; Yang, Y. Z.; Wang, L. Y.; Ma, X. C.; Zhang, X. B. *Tribol Lett* 2001, 10, 225.
6. Lim, D. S.; An, J. W.; Lee, H. J. *Wear* 2002, 252, 512.
7. Yang, Z.; Xu, H.; Li, M. K.; Shi, Y. L.; Huang, Y.; Li, H. L. *Thin Solid Films* 2004, 46, 686.

8. Chen, W. X.; Tu, J. P.; Wang, L. Y.; Gan, H. Y.; Xu, Z. D.; Zhang, X. B. *Carbon* 2003, 41, 215.
9. Cai, H.; Yuan, F. Y.; Xue, Q. J. *Mater Sci Eng Part A* 2004, 364, 94.
10. Chen, W. X.; Li, F.; Han, G.; Xia, J. B.; Wang, L. Y.; Tu, J. P.; Xu, Z. D. *Tribol Lett* 2003, 15, 275.
11. Zoo, Y. S.; An, J. W.; Lim, D. P.; Lim, D. D. *Tribol Lett* 2004, 16, 305.
12. Allaoui, A.; Bai, S.; Cheng, H. M.; Bai, J. B. *Compos Sci Technol* 2002, 62, 1993.
13. Jin, Z.; Pramoda, K. P.; Xie, G.; Goh, S. H. *Chem Phys Lett* 2001, 337, 43.
14. Zeng, J.; Saltysiak, B.; Johnson, W. S.; Schiraldi, D. A.; Kumar, S. *Compos B* 2004, 35, 173.
15. Mitchell, C. A.; Bahr, J. L.; Arepalli, S.; Tour, J. M.; Krishnamoorti, R. *Macromolecules* 2002, 35, 8825.
16. Viswanathan, G.; Chakrapani, N.; Yang, H.; Wei, B. Q.; Chung, H.; Cho, K.; Ryu, C. Y.; Ajayan, P. M. *J Am Chem Soc* 2003, 125, 9258.
17. Choi, H. J.; Zhang, K.; Lim, J. Y. *J Nanosci Nanotechnol* 2007, 7, 3400.
18. Kim, S. T.; Choi, H. J.; Hong, S. M. *Colloid Polym Sci* 2007, 285, 593.
19. Poa, C. H.; Silva, S. R. P.; Watts, P. C. P.; Hsu, W. K.; Kroto, H. W.; Walton, D. R. M. *Appl Phys Lett* 2002, 80, 3189.
20. Qian, D.; Dickey, E. C.; Andrews, R.; Rantell, T. *Appl Phys Lett* 2000, 76, 2868.
21. Schadler, L. S.; Giannaris, S. C.; Ajayan, P. M. *Appl Phys Lett* 1988, 73, 3842.
22. Yang, Z.; Dong, B.; Huang, Y.; Liu, L.; Yan, F. Y.; Li, H. L. *Mater Chem Phys* 2005, 94, 109.